Universal Semiclassical Coexistence in Classical Compression of Phase-Lifted Coherent States

Dimension-Normalized Contacts and a Matched High-Fidelity Boundary Layer

Lluis Eriksson

August 14, 2026

Abstract

Fix a nonzero dominant weight λ and let the highest weight grow along the ray $N\lambda$. We study the exact classical Shannon rate–distortion function of the invariant phase-lifted coherent orbit in $V_{N\lambda}$ under squared ambient Hilbert-space loss. The finite-N scalar formula is known; the new problem is the coupled large-weight and distortion limit. If $d_N = \dim V_{N\lambda}$, $\ell_N = \log d_N$, and $a = \dim_{\mathbb{C}}(G_{\mathbb{C}}/P_\lambda) + \frac{1}{2}$, we prove that the unique global origin-tangent contact, for all sufficiently large N, obeys

$$t_{c,N} = 2\ell_N + 2a \log \ell_N + \log(4\pi) - a + o(1), \quad D_{c,N} = \frac{a}{\ell_N} + o(\ell_N^{-1}),$$

and that its time-sharing slope is $\ell_N + a \log \ell_N + \log(2\sqrt{\pi}) + o(1)$. All root-system and Weyl leading constants cancel in these dimension variables. For fixed $0 < D \leq 1$ the exact unrestricted RDF satisfies $R_N(D)/\ell_N \to 1 - D$. On the noncommuting boundary scale $D = x/\ell_N$, the centered rate converges to an explicit two-branch profile:

$$\begin{cases} a \log(a/x) + \log(2\sqrt{\pi}) - a, & 0 < x \leq a, \\ \log(2\sqrt{\pi}) - x, & x \geq a. \end{cases}$$

We also identify the intervening soft-activation window, including an exact fixed-radius Legendre expansion. The proof combines a differentiated Weyl–Bessel saddle, global contact localization, and convex-envelope attainment. The result is classical rate–distortion for an embedded coherent-amplitude source, not quantum rate–distortion or a derivation of Born's rule.

1 Introduction

Coherent-state families connect compact representation theory, semiclassical geometry, and information theory. Their integer moments are controlled by Cartan products, while highest-weight scaling produces a classical localization regime. These ingredients are familiar separately: coherent moment extremality belongs to the generalized Lieb–Wehrl line [10, 17, 11], Weyl's formula governs the growth of irreducible representations [7], and entropy duality governs rate–distortion functions [4, 3]. What is not contained in those components is the convex-envelope phase transition of an *exact* coherent-orbit rate–distortion problem when the embedding itself becomes semiclassical.

The finite-dimensional starting point was established in [6]. For a fixed irreducible representation, its Cartan-product Laplace theorem reduces arbitrary standard-Borel memories and arbitrary square-integrable Euclidean reports to a scalar lower convex envelope. This paper studies a different question: fix the abstract projective orbit but replace λ by $N\lambda$ and send N to infinity. The orbit's embedding sharpens, its Hilbert dimension diverges, and the scalar envelope develops three separated regimes:

1. a soft activation at field $\ell_N + a \log \ell_N + O(1)$;
2. a global origin-tangent contact at twice the leading field;
3. a high-fidelity layer $D\ell_N = O(1)$ in which the curved coherent branch and the time-sharing line remain simultaneously visible.

Our principal finding is universality in the correct coordinate. If one works in $\log N$, the leading orbit dimension and the Weyl constant appear. If one instead uses the observable Hilbert dimension $d_N = \dim V_{N\lambda}$, all representation-specific constants cancel from the contact through order one. The complete boundary profile then depends only on

$$a = p + \frac{1}{2}, \qquad p = \dim_{\mathbb{C}}(G_{\mathbb{C}}/P_\lambda),$$

half the real dimension of the phase-lifted source.

General high-resolution results for random variables on manifolds provide power-law and dimensional bounds [9, 12, 15]. Here the object is different: the ambient embedding changes with N, the exact finite-N RDF is retained, and the critical distortion is of order $1/\log d_N$, rather than being obtained by first fixing a source and then taking distortion to zero.

The tensor-power classical limit itself is also established territory in Berezin–Toeplitz and semiclassical free-energy theory [16, 2]. The recent $SU(2)$ coherent-state majorization theorem of Abreu [1] is a particularly close geometric neighbor, but it contains neither a Shannon RDF nor the contact and boundary-layer problem treated here. At $N = 1$, the $SU(2)$ phase lift is the unit sphere in $\mathbb{C}^2 \simeq \mathbb{R}^4$, so its finite-dimensional RDF is also the radius-one, four-real-dimensional case of the exact sphere result of Dytso and Cardone [5]. Visible quantum compression [8] is operationally different from the classical Euclidean reporting problem studied below.

Claims boundary. We prove eventual uniqueness only for the *global minimizing origin-tangent contact*. We do not claim that every finite-N radial stationary equation has one root, nor do we exclude every metastable radial branch. We make no statement at fixed zero distortion, where every finite-N continuous orbit has infinite exact-reproduction rate.

2 Finite-dimensional input and notation

Let G be a compact connected semisimple group and let λ be a nonzero dominant integral weight. For each integer $N \geq 1$, let $V_{N\lambda}$ be the irreducible unitary representation of highest weight $N\lambda$, with unit highest-weight vector v_N. The phase-lifted coherent orbit is

$$\mathcal{M}_N = \{e^{i\theta}\pi_N(g)v_N : g \in G,\ \theta \in [0, 2\pi)\},$$

equipped with invariant probability μ_N. We regard $V_{N\lambda}$ as a real Hilbert space with squared Euclidean loss.

For a random $X_N \sim \mu_N$, an encoder may use an arbitrary standard-Borel memory Z and a square-integrable report $\widehat{X}(Z)$. The classical RDF is

$$R_N(D) = \inf\{I(X_N; Z) : \mathbb{E}\|X_N - \widehat{X}(Z)\|^2 \leq D\}.$$

No restriction to coherent reports is imposed.

Write

$$d_{m,N} = \dim V_{mN\lambda}, \qquad d_N = d_{1,N},$$

and define

$$L_N(t) = \sum_{m=0}^{\infty} \frac{(t^2/4)^m}{(m!)^2 d_{m,N}}, \qquad K_N(t) = \log L_N(t), \tag{1}$$

$$j_N(b) = \sup_{t\geq 0}\{tb - K_N(t)\}, \qquad g_N(u) = j_N(\sqrt{u}). \tag{2}$$

We import the following exact result, with attribution explicit because the finite-N theorem is not the novelty of this paper.

Theorem 2.1 (Exact coherent-orbit RDF, [6])**.** *For every N and $0 \leq D \leq 1$,*

$$\boxed{R_N(D) = (\mathrm{co}\, g_N)(1-D).} \tag{2.3}$$

Every exposed point is attained by a covariant exponential posterior. Every nonexposed chord is attained by revealing an independent binary time-sharing flag. The converse allows arbitrary standard-Borel memories and arbitrary square-integrable reports.

The theorem follows from the Cartan-component identity

$$\int_G |\langle w, \pi_N(g) v_N\rangle|^{2m}\, \mathrm{d}g = \frac{\|P_{mN\lambda} w^{\otimes m}\|^2}{d_{m,N}} \leq \frac{\|w\|^{2m}}{d_{m,N}},$$

with equality classified by coherent rays, followed by conditional least squares and entropy duality. We use its scalar conclusion, not a restricted coding ansatz.

Let

$$\Phi_\lambda^+ = \{\alpha > 0 : \langle \lambda, \alpha^\vee\rangle > 0\}, \qquad p = |\Phi_\lambda^+|, \qquad a = p + \frac{1}{2}, \qquad \ell_N = \log d_N.$$

Then $p = \dim_{\mathbb{C}}(G_{\mathbb{C}}/P_\lambda)$. We assume $p \geq 1$ throughout.

3 A differentiated Weyl–Bessel saddle

The asymptotic analysis must be simultaneous in the Cartan index m and the scaling parameter N. A pointwise use of Weyl's formula at fixed m would not control the Bessel saddle $m \asymp t$.

3.1 Exact Weyl factorization

For each active root define

$$c_\alpha = \frac{\langle \lambda, \alpha^\vee\rangle}{\langle \rho, \alpha^\vee\rangle} > 0.$$

Inactive roots contribute one, so Weyl's formula is the exact product

$$d_{m,N} = \prod_{\alpha\in\Phi_\lambda^+} (1 + mNc_\alpha).$$

Consequently, uniformly for all integers $m \geq 1$,

$$\frac{1}{d_{m,N}} = \frac{1}{d_N} m^{-p} \prod_{\alpha\in\Phi_\lambda^+} \frac{m(1+Nc_\alpha)}{1+mNc_\alpha} = \frac{1}{d_N} m^{-p}\{1 + O(N^{-1})\}.$$

The uniformity in m is elementary and crucial.

Put $H_N(t) = L_N(t) - 1$ and

$$B_p = \frac{2^p}{\sqrt{2\pi}}.$$

Lemma 3.1 (Uniform differentiated saddle)**.** *Fix $c > 0$. Uniformly for $t \geq c\ell_N$,*

$$\log H_N(t) = t - a \log t - \ell_N + \log B_p + O(t^{-1} + N^{-1}), \tag{3}$$

$$(\log H_N)'(t) = 1 - \frac{a}{t} + O(t^{-2} + (Nt^2)^{-1}), \tag{4}$$

$$(\log H_N)''(t) = \frac{a}{t^2} + O(t^{-3} + (Nt^3)^{-1}). \tag{5}$$

Proof. Let

$$T_p(t) = \sum_{m \geq 1} \frac{(t^2/4)^m}{(m!)^2 m^p}.$$

Put $z = t/2$ and introduce the Bessel law

$$\Pr(M_z = m) = \frac{z^{2m}}{(m!)^2 I_0(2z)}, \qquad m \geq 0.$$

It is the law of either of two independent Poisson(z) variables conditioned to be equal. Define $f_p(0) = 0$ and $f_p(m) = m^{-p}$ for $m \geq 1$. Then

$$T_p(2z) = I_0(2z)\, \mathbb{E} f_p(M_z). \tag{6}$$

We record the moment calculation because two differentiated orders are used later. From

$$\mathbb{E} M_z = z \frac{I_1(2z)}{I_0(2z)}, \qquad \mathrm{Var}(M_z) = \frac{z}{2} \frac{\mathrm{d}}{\mathrm{d}z} \mathbb{E} M_z$$

and the standard Debye expansions [13, 14],

$$\begin{aligned} \mathbb{E}(M_z - z) &= -\frac{1}{4} + O(z^{-1}), \\ \mathbb{E}(M_z - z)^2 &= \frac{z}{2} + O(1). \end{aligned} \tag{7}$$

Repeated application of $(z/2)\partial_z$ to $\log I_0(2z)$ bounds every fixed higher cumulant by $O(z)$. Chernoff's inequality for the conditioned Poisson pair gives exponentially small tails outside $|M_z - z| \leq \sqrt{z} \log z$. Taylor expansion of f_p through fourth order on that window, with equation (7) and the corresponding third and fourth central moments, therefore yields

$$\mathbb{E} f_p(M_z) = z^{-p} \left\{ 1 + \frac{p(p+2)}{4z} + O(z^{-2}) \right\}. \tag{8}$$

The same calculation after inserting $(2M_z)^j$, $j = 1, 2$, proves the differentiated form

$$\partial_t^j \left[\frac{e^{-t} t^a T_p(t)}{B_p} - 1 - \frac{A_p}{t} \right] = O(t^{-2-j}), \qquad j = 0, 1, 2. \tag{9}$$

where $A_p = p(p+2)/2 + 1/8$. Thus no differentiation of an unspecified $o(1)$ is being used. Taking logarithms in equation (9) gives

$$\begin{aligned} \log T_p(t) &= t - a \log t + \log B_p + A_p/t + O(t^{-2}), \\ (\log T_p)'(t) &= 1 - a/t - A_p/t^2 + O(t^{-3}), \\ (\log T_p)''(t) &= a/t^2 + 2A_p/t^3 + O(t^{-4}). \end{aligned} \tag{10}$$

It remains to track the Weyl correction without hiding its m-independent part. The factor in section 3.1 splits exactly as

$$\prod_\alpha \frac{m(1 + Nc_\alpha)}{1 + mNc_\alpha} = C_N Q_{m,N}, \quad C_N = \prod_\alpha \left(1 + \frac{1}{Nc_\alpha}\right), \quad Q_{m,N} = \prod_\alpha \left(1 + \frac{1}{mNc_\alpha}\right)^{-1}. \tag{11}$$

Hence $\log C_N = O(N^{-1})$ and, if $\nu_{p,t}$ denotes the probability law on $m \geq 1$ proportional to the summands of $T_p(t)$,

$$H_N(t) = d_N^{-1} C_N T_p(t)\, \mathbb{E}_{\nu_{p,t}} Q_{M,N}. \tag{12}$$

On the Bessel window, $Q_{m,N} = 1 + O((Nm)^{-1})$ and its first two discrete differences are respectively $O((Nm^2)^{-1})$ and $O((Nm^3)^{-1})$. The moment bounds above then give, uniformly for $t \geq c\ell_N$,

$$\begin{aligned} \mathbb{E}_\nu Q_{M,N} &= 1 + O((Nt)^{-1}), \\ \mathbb{E}_{\nu^Q} M - \mathbb{E}_\nu M &= O((Nt)^{-1}), \\ \mathrm{Var}_{\nu^Q}(M) - \mathrm{Var}_\nu(M) &= O((Nt)^{-1}), \end{aligned} \tag{13}$$

where $\nu^Q(m) \propto Q_{m,N}\nu(m)$. For completeness, exponential-family differentiation now gives the exact identities

$$\begin{aligned} \partial_t \log \mathbb{E}_\nu Q &= \frac{2}{t}\{\mathbb{E}_{\nu^Q} M - \mathbb{E}_\nu M\}, \\ \partial_t^2 \log \mathbb{E}_\nu Q &= -\frac{2}{t^2}\{\mathbb{E}_{\nu^Q} M - \mathbb{E}_\nu M\} + \frac{4}{t^2}\{\mathrm{Var}_{\nu^Q} M - \mathrm{Var}_\nu M\}. \end{aligned} \tag{14}$$

Using equations (10) and (12) to (14) produces errors $O(t^{-1} + N^{-1})$, $O(t^{-2} + (Nt^2)^{-1})$, and $O(t^{-3} + (Nt^3)^{-1})$ at logarithmic derivative orders zero, one, and two, respectively. This proves equations (3) to (5) and makes explicit why the $O(N^{-1})$ part disappears after logarithmic differentiation. □

One coarse consequence is the logarithmic transition

$$\frac{K_N(c\ell_N)}{\ell_N} \longrightarrow (c-1)_+, \qquad c > 0,$$

locally uniformly away from $c = 1$.

4 The soft-activation window

The normalizer first becomes order one well before the global contact. This intermediate regime supplies a full three-scale theorem and prevents an incorrect direct jump from the Gaussian origin to the contact field.

Theorem 4.1 (Soft activation)**.** *Fix $y \in \mathbb{R}$ and set*

$$t_N(y) = \ell_N + a \log \ell_N + y.$$

Then

$$H_N(t_N(y)) \longrightarrow B_p e^y, \tag{15}$$

$$K_N(t_N(y)) \longrightarrow \log(1 + B_p e^y), \tag{16}$$

$$K_N'(t_N(y)) \longrightarrow \vartheta_y := \frac{B_p e^y}{1 + B_p e^y}. \tag{17}$$

More precisely, define the activation-normalized field $\tau_N(y)$ by

$$H_N(\tau_N(y)) = B_p e^y.$$

Then $\tau_N(y) = \ell_N + a\log \ell_N + y + o(1)$ *and*

$$K_N'(\tau_N(y)) = \vartheta_y \left(1 - \frac{a}{\tau_N(y)}\right) + o(\ell_N^{-1}), \tag{18}$$

$$j_N(K_N'(\tau_N(y))) = \vartheta_y \ell_N + a\vartheta_y \log \ell_N + \vartheta_y(y-a) - \log(1 + B_p e^y) + o(1). \tag{19}$$

Equivalently, for every fixed $b \in (0,1)$, *the exact conjugate field and cost obey*

$$t_N(b) = \ell_N + a\log \ell_N + \log \frac{b}{B_p(1-b)} + o(1), \tag{20}$$

$$j_N(b) = b\ell_N + ab\log \ell_N + b\log b + (1-b)\log(1-b) - b\log B_p + o(1). \tag{21}$$

Proof. The first three limits follow directly from equation (3) and $K_N' = H_N'(1+H_N)^{-1}$. Monotonicity of H_N gives the unique field in theorem 4.1; equation (3) then gives its expansion. At that field, the amplitude of H_N is exact, so the $O(\log \ell_N/\ell_N)$ correction that would otherwise be amplified by multiplication by t is absent. Using equations (4) and (18) and $j = tb - K$ yield equation (19). Solving for fixed b requires one further order. Put $\vartheta_N = H_N(t)/(1 + H_N(t))$. Uniformly for b in compact subsets of $(0,1)$,

$$b = \vartheta_N \left(1 - \frac{a}{t}\right) + O(t^{-2}), \qquad \vartheta_N = b + \frac{ab}{\ell_N} + o(\ell_N^{-1}).$$

Moreover,

$$t = \ell_N + a\log t + \log \frac{\vartheta_N}{1-\vartheta_N} - \log B_p + o(1).$$

Since $K_N(t) = -\log(1-\vartheta_N)$ and $tb = t\vartheta_N - a\vartheta_N + o(1)$, substitution gives

$$j_N(b) = \vartheta_N \ell_N + a\vartheta_N \log \ell_N + \vartheta_N \log \frac{\vartheta_N}{1-\vartheta_N} - \vartheta_N \log B_p - a\vartheta_N + \log(1-\vartheta_N) + o(1).$$

Here $\ell_N(\vartheta_N - b) = ab + o(1)$ cancels $-a\vartheta_N = -ab + o(1)$. Letting $\vartheta_N \to b$ in the remaining order-one terms proves equations (20) and (21). This cancellation is why no extra $-ab$ occurs in equation (21). $\square$

Remark 4.2 (Why the centering matters)**.** *The leading limits at the naive field* $t_N(y)$ *are valid, but one may not insert* $K_N'(t_N(y)) = \vartheta_y + o(1)$ *into* $tK' - K$ *and claim an* $O(1)$ *expansion: an* $O(\log \ell_N/\ell_N)$ *error in* K' *is multiplied by* $t \asymp \ell_N$. *The exact activation coordinate theorem 4.1, or the fixed-b formula equation (21), removes this ambiguity.*

5 Global contact and dimension-universal constants

Define the best origin-supported slope

$$\rho_N = \inf_{0<b<1} \frac{j_N(b)}{b^2}.$$

The quotient tends to d_N at the origin and diverges at $b \uparrow 1$. The trial field $t = 2\ell_N$ has $h_N(t) = O(\ell_N) < d_N$, so for all sufficiently large N the infimum is attained at a positive interior field. Parameterize $b = K_N'(t)$ and put

$$h_N(t) = \frac{tK_N'(t) - K_N(t)}{K_N'(t)^2}.$$

Direct differentiation gives the exact identity

$$h_N'(t) = \frac{K_N''(t)}{K_N'(t)^3}\{2K_N(t) - tK_N'(t)\}.$$

The denominator is the third power; replacing it by a square would be an algebraic error, though it would not change the stationary equation.

Lemma 5.1 (Global localization)**.** *Every global minimizer $t_{c,N}$ of h_N satisfies*

$$\frac{t_{c,N}}{\ell_N} \longrightarrow 2, \qquad K_N'(t_{c,N}) \longrightarrow 1.$$

For all sufficiently large N, the global minimizing contact is unique. This does not assert uniqueness of all stationary roots outside the global contact window.

Proof. For $t = c\ell_N$ with $c > 1$ fixed, H_N is a positive power of d_N. When c is bounded away from one it is in fact much larger than ℓ_N, so replacing $\log(1 + H_N)$ by $\log H_N$ incurs $o(1/\ell_N)$ in the calculation of h_N. Uniformly on compact subsets of $(1, \infty)$,

$$h_N(c\ell_N) = \ell_N + a \log \ell_N + F_a(c) + o(1),$$

where

$$F_a(c) = a \log c + \frac{2a}{c} - a - \log B_p.$$

Since $F_a'(c) = a(c - 2)/c^2$, its unique minimum is $c = 2$.

It remains to exclude other field scales. For $t \leq (1 - \varepsilon)\ell_N$, the positive series and equation (3) make H_N exponentially small. Indeed, $d_{m,N} \geq d_N$ for $m \geq 1$, hence $H_N(t) \leq \{I_0(t) - 1\}/d_N \leq e^{t-\ell_N}$; the exact quotient is then exponentially larger than its value at $2\ell_N$ (bounded t follows from the quadratic origin expansion). In the soft window, equation (21) gives $j_N(b)/b^2 = \ell_N/b + O(\log \ell_N)$, strictly larger than the candidate slope for every radius bounded away from one. Radii tending to zero are excluded by combining the quadratic origin $h_N(0+) = d_N$ with the subactivation estimate.

It remains to control the full transition window $t/\ell_N \to 1$. Put $S = H_N(t)$ and $A = (\log H_N)'(t)$. If $S \to 0$, the exact formulas give $h_N(t) \sim t/S$, hence $h_N/\ell_N \to \infty$. If S stays bounded away from both zero and infinity, then along every convergent subsequence $b_N \to S/(1 + S) < 1$, and the fixed-radius expansion gives $h_N/\ell_N \to 1/b_N > 1$. Finally suppose $S \to \infty$ and define

$$\bar{h}_N = \frac{tA - \log S}{A^2}.$$

With $\delta = S^{-1}$, direct algebra gives the exact difference

$$h_N - \bar{h}_N = \frac{tA\delta - (2\delta + \delta^2)\log S - (1 + \delta)^2 \log(1 + \delta)}{A^2}. \tag{5.5}$$

Because $t \sim \ell_N$, $\log S = o(\ell_N)$, and $A \to 1$, this difference is nonnegative for all sufficiently large N. Meanwhile the saddle expansion gives

$$\bar{h}_N = \ell_N + a \log \ell_N + a - \log B_p + o(1).$$

Its order-one constant exceeds the $c = 2$ constant by $a(1 - \log 2) > 0$. Thus no sequence in the transition window can minimize globally. If $t/\ell_N \to \infty$, equation (3) gives an excess $a \log(t/\ell_N) \to \infty$. Thus every global minimizer lies in the $c = 2 + o(1)$ window.

There $H_N \gg \ell_N$, so logistic corrections are uniformly negligible, and equations (4) and (5) gives

$$K_N'(t) - tK_N''(t) = 1 - \frac{2a}{t} + o(t^{-1}) > 0.$$

Hence $2K_N - tK_N'$ is strictly increasing throughout the localized window. Together with section 5, this proves uniqueness of the global minimizing contact for all sufficiently large N. ∎

Theorem 5.2 (Universal global contact)**.** *Let $b_{c,N} = K_N'(t_{c,N})$ and $D_{c,N} = 1 - b_{c,N}^2$. Then*

$$t_{c,N} = 2\ell_N + 2a\log\ell_N + \log(4\pi) - a + o(1), \tag{22}$$

$$b_{c,N} = 1 - \frac{a}{t_{c,N}} + o(\ell_N^{-1}), \tag{23}$$

$$D_{c,N} = \frac{a}{\ell_N} + o(\ell_N^{-1}), \tag{24}$$

$$\rho_N = \ell_N + a\log\ell_N + \log(2\sqrt{\pi}) + o(1). \tag{25}$$

The rate at the positive end of the coexistence face is

$$j_N(b_{c,N}) = \ell_N + a\log\ell_N + \log(2\sqrt{\pi}) - a + o(1).$$

Proof. At an interior minimum, section 5 gives the contact equation

$$2K_N(t_{c,N}) = t_{c,N}K_N'(t_{c,N}).$$

By theorem 5.1, $H_N(t_{c,N}) \gg \ell_N$. Therefore

$$K_N(t) = t - a\log t - \ell_N + \log B_p + o(1),$$
$$K_N'(t) = 1 - a/t + o(t^{-1})$$

at contact. Substitution in section 5 gives

$$t_{c,N} = 2\ell_N + 2a\log t_{c,N} - 2\log B_p - a + o(1).$$

Since $t_{c,N}/\ell_N \to 2$ and $B_p = 2^p/\sqrt{2\pi}$, the identity $a - p = 1/2$ yields

$$2a\log 2 - 2\log B_p = \log(4\pi),$$

which proves equation (22). Equations equations (23) and (24) follow from the derivative saddle. At contact, $j_N = tb - K = tb/2$, hence $\rho_N = t/(2b)$; expanding $1/b$ proves equation (25) and theorem 5.2. ∎

Proposition 5.3 (Exact convex-envelope gluing)**.** *For all sufficiently large N, put $u_{c,N} = b_{c,N}^2$. Then*

$$(\operatorname{co} g_N)(u) = \begin{cases} \rho_N u, & 0 \le u \le u_{c,N}, \\ g_N(u), & u_{c,N} \le u < 1. \end{cases}$$

Proof. Global minimality in section 5 gives $g_N(u) \ge \rho_N u$ for every u. At contact, $g_N(u_{c,N}) = \rho_N u_{c,N}$ and

$$g_N'(u_{c,N}) = \frac{t_{c,N}}{2b_{c,N}} = \rho_N.$$

Write $b = \sqrt{u}$ and let $t = j_N'(b)$, so that $b = K_N'(t)$ and $j_N''(b) = 1/K_N''(t)$. Direct differentiation gives

$$g_N''(u) = \frac{b - tK_N''(t)}{4b^3K_N''(t)}.$$

Here $K_N''(t) > 0$, since it is the variance of a nondegenerate tilted overlap law. Uniformly on the post-contact branch, equations (4) and (5) and $H_N(t) \to \infty$ give

$$b - tK_N''(t) = K_N'(t) - tK_N''(t) = 1 - \frac{2a}{t} + O\Big(t^{-2} + (Nt^2)^{-1} + tH_N(t)^{-1}\Big) > 0$$

for all sufficiently large N. Thus $g_N'' > 0$ on $[u_{c,N}, 1)$. Hence the function equal to $\rho_N u$ before contact and $g_N(u)$ after contact is convex and lies below g_N, so it is a convex minorant. Conversely, every convex minorant lies below the chord from $(0,0)$ to $(u_{c,N}, g_N(u_{c,N}))$ on the first interval and lies below g_N on the second. This proves theorem 5.3 and explicitly rules out a later chord lowering the high-fidelity branch. ☐

6 Macroscopic law and matched boundary layer

Theorem 6.1 (Macroscopic exact-RDF limit)**.** *For every fixed* $0 < D \leq 1$*,*

$$\boxed{\frac{R_N(D)}{\log d_N} \longrightarrow 1 - D.}$$

The convergence is uniform on $D \in [\delta, 1]$ *for every* $\delta > 0$*. Equivalently, since* $\ell_N = p \log N + O(1)$*,*

$$\frac{R_N(D)}{\log N} \longrightarrow p(1 - D).$$

Proof. By theorem 5.3, the lower convex envelope equals the contact line on $0 \leq u \leq b_{c,N}^2$, and every such point is attained by the time-sharing construction in theorem 2.1. For fixed $D > 0$, equation (24) gives $1 - D < b_{c,N}^2$ eventually, so

$$R_N(D) = \rho_N(1 - D).$$

Now use equation (25). At $D = 1$ both sides vanish exactly. The point $D = 0$ is excluded because $R_N(0) = +\infty$ for every finite-N continuous orbit. ☐

The macroscopic line hides the transition. Its complete nontrivial remnant appears when $D\ell_N$ stays finite.

Theorem 6.2 (Matched high-fidelity boundary layer)**.** *Fix* $x > 0$ *and put* $D_N = x/\ell_N$*. Then*

$$R_N(D_N) - \ell_N - a \log \ell_N \longrightarrow \mathcal{H}_a(x),$$

locally uniformly for $x \in (0, \infty)$*, where*

$$\boxed{\mathcal{H}_a(x) = \begin{cases} a \log(a/x) + \log(2\sqrt{\pi}) - a, & 0 < x \leq a, \\ \log(2\sqrt{\pi}) - x, & x \geq a. \end{cases}}$$

The branches have matching value and derivative at $x = a$*.*

Proof. For the deterministic coherent-radius branch set $b = \sqrt{1 - x/\ell_N}$. The saddle equation $b = K_N'(t)$ and equation (4) give

$$t = \frac{2a\ell_N}{x} + O(1).$$

Substitution in $j_N(b) = tb - K_N(t)$ yields

$$g_N(1 - x/\ell_N) = \ell_N + a \log \ell_N + a \log(a/x) + \log(2\sqrt{\pi}) - a + o(1).$$

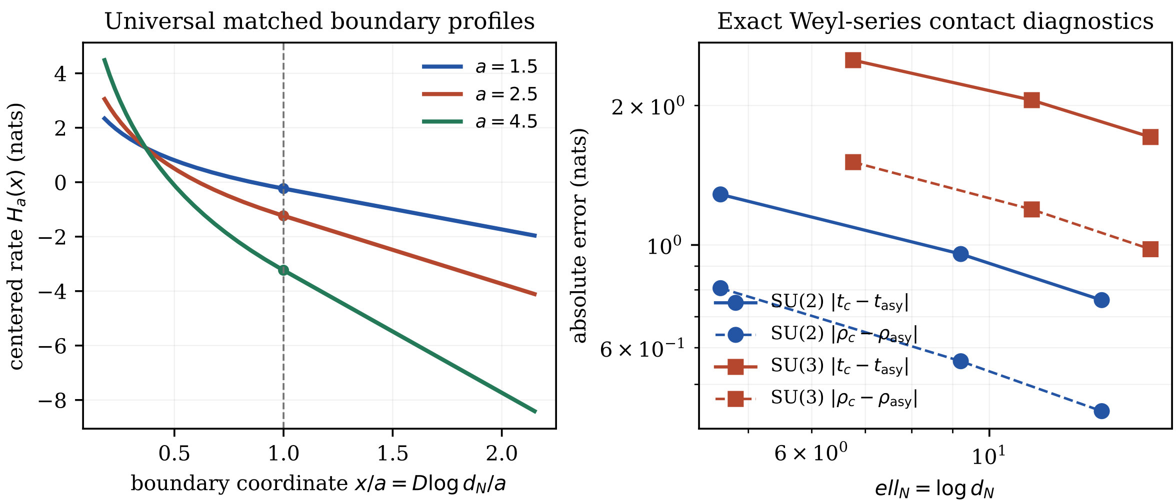

Figure 1: Left: the universal centered boundary profile $\mathcal{H}_a(x)$, with the horizontal coordinate normalized by its contact value a. Dots mark the tangencies. Right: bounded deterministic diagnostics from the exact Weyl series for symmetric powers of $SU(2)$ and $SU(3)$. Slow convergence is expected because the theorem contains a $\log\log d_N$ correction. Numerics illustrate the analytic theorem but are not used in its proof.

The cancellation uses again $a - p = 1/2$.

By equation (24), contact occurs at $x = a + o(1)$. For $x > a$, the requested point lies on the origin-to-contact face, and equation (25) gives

$$R_N(x/\ell_N) = \rho_N(1 - x/\ell_N) = \ell_N + a\log\ell_N + \log(2\sqrt{\pi}) - x + o(1).$$

For $0 < x < a$, the point lies beyond contact toward high fidelity, so theorem 5.3 makes the high-fidelity branch the exact lower hull and gives section 6. Both the raw-branch expansion and the contact-line expansion are uniform for x in any compact subset of $(0, \infty)$. The exact selector changes at $x_{c,N} = \ell_N D_{c,N} \to a$, and the two limiting expressions agree at a; hence their piecewise selection converges uniformly on every such compact set. At $x = a$, both formulas give $\log(2\sqrt{\pi}) - a$, and both derivatives equal -1. $\square$

The difference between the curved branch and the continuation of the tangent line is

$$a\{-\log(x/a) - 1 + x/a\} \geq 0,$$

with equality only at contact.

7 Examples

7.1 Symmetric powers of $SU(q)$

For $G = SU(q)$ and $\lambda = \omega_1$,

$$V_{N\omega_1} = \mathrm{Sym}^N(\mathbb{C}^q), \qquad d_N = \binom{N+q-1}{q-1}, \qquad p = q-1, \qquad a = q - \frac{1}{2}.$$

Thus the macroscopic law is universal after division by $\log\binom{N+q-1}{q-1}$, while the boundary contact occurs at $D_c \log d_N \to q - 1/2$.

For $SU(2)$, the scalar normalizer has the exact integral fixture

$$L_N(t) = \sum_{m\geq 0} \frac{(t^2/4)^m}{(m!)^2(mN+1)} = \int_0^1 I_0(tx^{N/2})\,\mathrm{d}x.$$

This follows by inserting $(mN+1)^{-1} = \int_0^1 x^{mN}\mathrm{d}x$ term by term. It provides a transparent one-dimensional check of every scale in the theorem.

For $SU(3)$,

$$d_{m,N} = \frac{(mN+1)(mN+2)}{2}, \qquad p = 2, \qquad a = \frac{5}{2}.$$

The exact positive series remains inexpensive even for symbolic values of N spanning many orders of magnitude.

7.2 Cartan powers of Slater-determinant orbits

For $G = SU(n)$ and $\lambda = \omega_k$, the abstract projective coherent orbit is $\mathrm{Gr}_{\mathbb{C}}(k,n)$ and

$$p = k(n-k), \qquad a = k(n-k) + \frac{1}{2}.$$

At $N = 1$ the coherent vectors are unit Slater determinants in $\Lambda^k\mathbb{C}^n$. The ray $N\omega_k$ is the Nth Cartan-power embedding of the same projective orbit. The present theorem applies to this embedding sequence. It should not be misread as an assertion that a single physical fermionic Hilbert space has changed particle number without changing the representation.

8 Reproducibility and numerical scope

The accompanying script evaluates equation (1) by a positive recurrence, computes K_N' exactly from the normalized weights, and solves the global contact equation

$$2K_N(t) - tK_N'(t) = 0$$

inside the analytically localized window. It includes two exact Weyl sequences:

family	$d_{m,N}$	(p,a)
$SU(2)$ symmetric powers	$mN+1$	$(1, 3/2)$
$SU(3)$ symmetric powers	$(mN+1)(mN+2)/2$	$(2, 5/2)$

The replay is deterministic, uses no Monte Carlo, and finishes in less than one second on the reference machine. The JSON output records the exact contact residual, distortion, slope, asymptotic predictions, and convergence errors. Figure 1 is generated from that frozen output and the closed form theorem 6.2. These checks diagnose constants and code paths; they do not replace the proofs.

9 Scope, novelty boundary, and open problems

The theorem concerns a sequence of *classical* random vectors supported on phase-lifted coherent orbits. Mutual information and rates are classical. It is not quantum rate–distortion, a quantum channel-capacity theorem, a click-only hidden-variable simulation, or a derivation of Born probabilities.

The following ingredients are prior machinery and are not claimed as new: Weyl's dimension formula, Cartan components, integer-index coherent moment extremality, Bessel asymptotics, entropy variational duality, and the exact finite-N RDF of [6]. The contribution is the coupled highest-weight asymptotic theorem: its global contact localization, dimension-universal constants, soft-activation expansion, dimension-normalized exact-RDF limit, and matched boundary profile.

Three boundaries are important.

1. Eventual uniqueness is proved for the global minimizing origin tangent only. Other finite-N stationary roots are not classified.

2. The limit theorem 6.1 requires fixed $D > 0$. The boundary theorem handles $D \asymp 1/\log d_N$, but exact zero distortion remains infinite.

3. The abstract orbit is fixed while its Cartan embedding changes. Results for a fixed representation followed by $D \downarrow 0$ are a different asymptotic problem.

Natural next questions include third-order contact expansions retaining the root-system-dependent N^{-1} terms, moderate deviations between the soft window and global contact, and extensions to sign-quotiented or projective losses whose posterior-mean bodies differ from the phase-lifted orbitope.

10 Conclusion

Highest-weight scaling turns the exact coherent-orbit compression problem into a universal phase diagram. The normalizer first activates at $\ell_N + a \log \ell_N + O(1)$, but the best time-sharing tangent waits until a field twice as large to leading order. The critical distortion shrinks as a/ℓ_N, the fixed-distortion RDF becomes the line $(1 - D)\ell_N$, and a matched $D\ell_N$ boundary layer retains the curved coherent branch and its tangent in one explicit profile. Writing the result in terms of the actual Hilbert dimension removes every Weyl leading constant and leaves only half the real source dimension. The universality is therefore not an artifact of one group or one orbit: it is the common semiclassical signature of the exact Cartan-product rate–distortion mechanism.

Data and code availability

The source package contains the LaTeX manuscript, bibliography, vector figure and its generator, the bounded verification script, and frozen JSON output. No external data set is used. All floating-point values are diagnostic.

Use of AI tools

AI tools assisted with literature discovery, algebraic replay, adversarial checking, drafting, and layout inspection. The named author takes responsibility for the claims, proofs, citations, and release artifacts. No peer review or independent scientific validation is claimed.

References

[1] Luis Daniel Abreu. *Isospectral Majorization and Isoperimetric Inequalities for Coherent States on the Bloch Sphere*. 2026. arXiv: 2608.12248 [quant-ph].

[2] Zied Ammari, Michele Correggi, Marco Falconi, and Raphaël Gautier. *Semiclassical Limit of Entropies and Free Energies*. 2025. arXiv: 2510.15777 [math-ph].

[3] Thomas M. Cover and Joy A. Thomas. *Elements of Information Theory*. 2nd ed. Hoboken: Wiley, 2006. DOI: 10.1002/047174882X.

[4] Imre Csiszár. “On an Extremum Problem of Information Theory”. In: *Studia Scientiarum Mathematicarum Hungarica* 9 (1974), pp. 57–61.

[5] Alex Dytso and Martina Cardone. “Uniform Distribution on $(n-1)$-Sphere: Rate-Distortion under Squared Error Distortion”. In: *2024 IEEE International Symposium on Information Theory*. 2024, pp. 873–878. DOI: 10.1109/ISIT57864.2024.10619427. arXiv: 2401.04248 [cs.IT].

[6] Lluis Eriksson. “Exact Classical Rate–Distortion for Phase-Lifted Generalized Coherent States: Cartan-Product Laplace Rigidity, Universal Radial Envelopes, and Slater-Determinant Transitions”. In: *Archive for Rigorous Research* (2026). ARR-2026-6XH6JAS5ZA934A6J, version 1. URL: https://arr-research.github.io/papers/ARR-2026-6XH6JAS5ZA934A6J/.

[7] William Fulton and Joe Harris. *Representation Theory: A First Course*. New York: Springer, 1991. DOI: 10.1007/978-1-4612-0979-9.

[8] Patrick Hayden, Richard Jozsa, and Andreas Winter. “Trading Quantum for Classical Resources in Quantum Data Compression”. In: *Journal of Mathematical Physics* 43.9 (2002), pp. 4404–4444. DOI: 10.1063/1.1497239. arXiv: quant-ph/0204038.

[9] Tsutomu Kawabata and Amir Dembo. “The Rate-Distortion Dimension of Sets and Measures”. In: *IEEE Transactions on Information Theory* 40.5 (1994), pp. 1564–1572. DOI: 10.1109/18.333868.

[10] Elliott H. Lieb. “Proof of an Entropy Conjecture of Wehrl”. In: *Communications in Mathematical Physics* 62 (1978), pp. 35–41. DOI: 10.1007/BF01940328.

[11] Elliott H. Lieb and Jan Philip Solovej. “Proof of the Wehrl-Type Entropy Conjecture for Symmetric SU(N) Coherent States”. In: *Communications in Mathematical Physics* 348 (2016), pp. 567–578. DOI: 10.1007/s00220-016-2596-9.

[12] Tamás Linder and Ram Zamir. “High-Resolution Source Coding for Non-Difference Distortion Measures: The Rate-Distortion Function”. In: *IEEE Transactions on Information Theory* 45.2 (1999), pp. 533–547. DOI: 10.1109/18.749001.

[13] NIST Digital Library of Mathematical Functions. *Modified Bessel Functions, Chapter 10*. https://dlmf.nist.gov/10. Accessed 2026-08-14.

[14] Frank W. J. Olver. *Asymptotics and Special Functions*. Wellesley: A K Peters, 1997.

[15] Erwin Riegler, Günther Koliander, and Helmut Bölcskei. “Lossy Compression of General Random Variables”. In: *Information and Inference: A Journal of the IMA* 12.3 (2023), pp. 1759–1829. DOI: 10.1093/imaiai/iaac035.

[16] Martin Schlichenmaier. “Berezin–Toeplitz Quantization for Compact Kähler Manifolds: A Review of Results”. In: *Advances in Mathematical Physics* 2010 (2010), p. 927280. DOI: 10.1155/2010/927280.

[17] Ayumu Sugita. “Proof of the Generalized Lieb–Wehrl Conjecture for Integer Indices Larger Than One”. In: *Journal of Physics A: Mathematical and General* 35.42 (2002), pp. L621–L626. DOI: 10.1088/0305-4470/35/42/105.